


# Key Areas of Gas Hydrates Study: Review

Olga Gaidukova <sup>1</sup>, Sergei Misyura <sup>1,2</sup> and Pavel Strizhak <sup>1,\*</sup> 

<sup>1</sup> Heat and Mass Transfer Laboratory, National Research Tomsk Polytechnic University, 634050 Tomsk, Russia; osy1@tpu.ru (O.G.); misura@itp.nsc.ru (S.M.)

<sup>2</sup> Kutateladze Institute of Thermophysics, Russian Academy of Sciences, 630090 Novosibirsk, Russia

\* Correspondence: pavelspa@tpu.ru

**Abstract:** Gas hydrates are widespread all over the world. They feature high energy density and are a clean energy source of great potential. The paper considers experimental and theoretical studies on gas hydrates in the following key areas: formation and dissociation, extraction and transportation technologies of natural methane hydrates, and ignition, and combustion. We identified a lack of research in more areas and defined prospects of further development of gas hydrates as a promising strategic resource. One of the immediate problems is that there are no research findings for the effect of sediments and their matrices on hydrate saturation, as well as on gas hydrate formation and dissociation rates. No mathematical models describe the dissociation of gas hydrates under various conditions. There is a lack of research into the renewal and improvement of existing technologies for the easier and cheaper production of gas hydrates and the extraction of natural gas from them. There are no models of gas hydrate ignition taking into account dissociation processes and the self-preservation effect.

**Keywords:** gas hydrates; dissociation; production; ignition; power engineering; strategic resource; clathrate



**Citation:** Gaidukova, O.; Misyura, S.; Strizhak, P. Key Areas of Gas Hydrates Study: Review. *Energies* **2022**, *15*, 1799. <https://doi.org/10.3390/en15051799>

Academic Editors: Nguyen Van Duc Long, Nicolas von Solms and Ingo Pecher

Received: 6 November 2021

Accepted: 24 February 2022

Published: 28 February 2022

**Publisher's Note:** MDPI stays neutral with regard to jurisdictional claims in published maps and institutional affiliations.



**Copyright:** © 2022 by the authors. Licensee MDPI, Basel, Switzerland. This article is an open access article distributed under the terms and conditions of the Creative Commons Attribution (CC BY) license (<https://creativecommons.org/licenses/by/4.0/>).

## 1. Introduction

Huge global stocks of gas hydrates provide an opportunity to reduce the volumes of coal and oil extraction and combustion [1]. Countries allocate large funds to search for this unique kind of gas and develop an extraction technology for it. Gas hydrates can be found worldwide. They feature high energy density and are a high-potential environmentally clean energy source [2]. So far, no country in the world has embarked on the commercial extraction of gas hydrates due to a lack of research in the field of extraction and ignition technologies of this alternative fuel.

Gas hydrates are solid crystalline compounds of low molecular weight gases (methane, ethane, butane, propane, etc.) and water. They look like snow or ice and share some physical properties with them [3]. They occur naturally from the contact of gas and water under certain conditions. Gas hydrates are stable at low temperatures and elevated pressures [4]. When the temperature increases and the pressure falls, gas hydrates dissociate into water and gas [5]. The most widespread hydrate-forming natural gas is methane [6]. Distinctive characteristics of natural gas hydrates include widespread occurrence, good stocks, high density, and high calorific value. The energy value of gas hydrates is comparable to that of bituminous oil and oil sands [7]. One cubic meter of a gas hydrate is equivalent to more than 160 m<sup>3</sup> of methane. Based on scientific estimates, natural hydrates may contain from 2000 to 5000 trillion m<sup>3</sup> of gas [8]. Thus, natural gas hydrates, especially marine gas hydrates, are seen as an innovative clean energy resource to replace fossil fuels in the 21st century [1].

There are artificial and natural gas hydrates [8]. Technogenic hydrates occur in systems of conventional natural gas production (in reservoirs, in well bores, etc.) and when gas is transported [9]. Gas hydrate formation is undesirable for the production and transportation

of conventional natural gas. This means that the prevention and elimination methods should be further improved [10]. Natural gas hydrates are dispersed or form agglomerates. This type of hydrate occurs in the Arctic and Antarctic, where the permafrost layer, more than 300 m in depth, creates conditions for hydrate formation [5].

At present, three major areas in scientific and development studies on gas hydrates [11] can be distinguished: formation and dissociation, extraction and transportation technologies of natural gas hydrates, and ignition and combustion. There have been major advances in the investigation of gas hydrates, yet the results of theoretical and experimental studies for the large-scale commercial introduction of gas hydrates in power production are scarce [12]. This study reviews the most significant achievements of the scientific community in the outlined research areas, with an additional focus on important problems remaining unsettled.

## 2. Historical Background of Gas Hydrates

The history of studying hydrates, dating back almost 200 years, can be broadly divided into three periods. The first one (1810–1934) is when artificial gas hydrates were first obtained under laboratory conditions. In his laboratory in 1810, Humphry Davy, a Royal Society scientist, made some remarkable advances and was the first to synthesize hydrates of chlorine. Later, Marcellin Berthelot, Paul-Ulrich Villard (France), Linus Pauling (the United States), and other researchers effectively synthesized a range of gas hydrates. The second period (1934–1993) marked the development of technologies for predicting and eliminating hydrates under commercial conditions [5]. In the early 1930s of the 20th century, technogenic hydrates disrupting natural gas flows were discovered in pipelines. This brought chemists and oil geologists to focus their attention on eliminating gas hydrate agglomerations in pipelines. At the same time, great resources of hydrate were found in permafrost regions and deep water [12]. In 1960, a combustible ice was discovered in Siberia [5]. In 1965, for the first time, scientists found deposits of gas hydrate in a permafrost region in Siberia [12]. In 1968, the Soviet researchers found deposits of gas hydrate when developing the Messoyakha gas field [5]. In the 1970s, gas hydrates were found in samples from the Alaska North Slope and on the Black Sea bed. The research findings from the 1980s resulted in identifying gas hydrates as a new methane source. In 1969, the United States researched gas hydrates and included them in a long-time governmental plan as a strategic energy source to be used nationally. In 1949, in the Gulf of Mexico, as part of the Deep Sea Drilling Project (DSDP), deep drilling operations were conducted, and 91.24 m of hydrate core samples were obtained from the seafloor, which confirmed the existence of gas hydrate deposits beneath the seafloor. The third period (from 1993 until the present), defined by the First International Congress on hydrates, is the main stage for devising a common scheme for hydrate development and research. At the same time, natural gas hydrates were located in Siberia, in the Mackenzie River delta, on the Alaska North Slope [13–15], in the Gulf of Mexico [16,17], the Gulf of Khambhat, the Sea of Japan [18,19], and on the northern slope of the South China Sea. Since 1990s, large-scale programs have been implemented to search for natural gas hydrates and develop artificial ones [20]. In 1998, Japan collaborated with Canadian specialists to conduct joint drilling in the Mackenzie Delta in the northwest of Canada. On 12 March 2013, methane was tapped from deep-sea gas hydrate near Aichi Prefecture. Japan became the first country to master the technology of gas hydrate extraction on a seabed. It aims to launch the large-scale commercial production of hydrates by 2027. The research and exploration of natural gas hydrates have broken new ground, and their development and commercialization have been recognized as an important goal [5]. Russia has large deposits of gas hydrates in Lake Baikal and the Black, Caspian, and Okhotsk Seas. The Yamburg, Bovanenkovo, Urengoy, and Messoyakha gas fields are worth mentioning as well [21]. Thousands of highly qualified specialists in many countries are currently addressing the problems of both natural and artificial gas hydrates.

### 3. Research Areas in the Field of Gas Hydrates

Table 1 summarizes some recent research activities on gas hydrates.

**Table 1.** Examples of research on gas hydrates.

Research Subject	Researchers	References
Formation and dissociation	Li X. Sen	[22,23]
	Zhao J.	[24]
	Collett T.S.	[25]
	Rossi F.	[26]
	Viana A.R.	[27]
	Misyura S.Y.	[28,29]
	Chen G.-J.	[30]
	Singh D.N.	[31]
	Vlasov V.A.	[32,33]
	Henry P.	[34]
	Salamatin A.N.	[35]
Extraction and transportation technologies	Kumar A.	[36]
	Wu Q.	[37,38]
	Teng Y.	[39]
	Al-Raoush R.I.	[40]
	Zhao J.	[41,42]
	Yang M.	[41]
	Jegen M.	[43]
	Guo B.	[44]
	Maruyama S.	[45]
	Chen Z.	[46,47]
	Wang B.	[48,49]
Combustion behavior	Falser S.	[50]
	Veluswamy H.P.	[51]
	Musakaev N.G.	[52–54]
	Yan D.	[55]
	Chien Y.C.	[56]
	Misyura S.Y.	[57–61]
	Yoshioka T.	[62]
	Liu J.	[63]
	Sirignano W.A.	[64]
	Dunn-Rankin D.	[65,66]
	Li Z.	[67]
Bar-Kohany T.	[68]	
Cui G.	[63,69–71]	
Wu F.-H.	[72]	

#### 3.1. Formation and Dissociation of Gas Hydrates

In gas hydrates, gas is completely in a solid, hydrated state. The presence of water and gas, specific pressure, and low temperatures are prerequisites for the formation of combustible ice [73]. Marine deposits and permafrost are the main locations of natural gas hydrate formation [23]. This involves a complex process of nucleation and hydrate accumulation in deposition matrices [24]. In the natural world, gas hydrates are usually dispersed in the pores of coarse-grained sediment [74]. The main portion of gas hydrates is located in porous media. However, the system of a porous medium has not been fully investigated, possibly due to the difficulty of visualizing hydrates inside a porous medium. An important overview on the formation of gas hydrates in porous media was considered by Clennell et al. [34]. They developed a conceptual model for the formation of gas hydrates in marine sediments [34]. The kinetics of gas hydrates in porous media was studied by Yousif et al. [75] using a one-dimensional isothermal model. Experimental studies on the formation of porous gas hydrates (methane and carbon dioxide) have been studied by Genov et al. [35]. Kumar et al. [36] researched the permeability and its effect on the

dissociation of gas hydrates in porous media. The formation of methane hydrate in a porous medium was considered by Zhang et al. [37]. Experimental research on methane hydrate formation in porous media based on low-field nuclear magnetic resonance has been studied by Zhan et al. [38]. Experimental studies of the formation of gas hydrates in a porous medium are challenging. Thus, numerical modeling is a useful tool in the study of this area [39,40,76].

Gas hydrate accumulations affect the characteristics of deposits, which, in turn, influence the decomposition of gas hydrates [22,25]. Three different natural gas hydrates were determined: cubic structure I (named sI) [77], cubic structure II (sII) [78], and a hexagonal structure H (sH) [79] (Figure 1). Structure I is made up of two little pentagonal dodecahedrons ( $5^{12}$ ) and six tetradecahedrons (14-hedrons,  $5^{12} \cdot 6^2$ ). Such a structure evolves in the presence of guest molecules (carbon dioxide or methane). Structure II contains sixteen cages of  $5^{12}$  and eight tetradecahedrons (16-hedrons,  $5^{12} \cdot 6^4$ ). This structure has hydrogen or propane as the guest molecules. The type H structure is based on three cells of  $5^{12}$ , two irregular dodecahedrons ( $4^3 \cdot 5^6 \cdot 6^3$ ), and one cell of  $5^{12} \cdot 6^8$ . The type H structure may contain guest molecules whose diameters exceed that of the compounds contained in the other structures (pentane) [26].

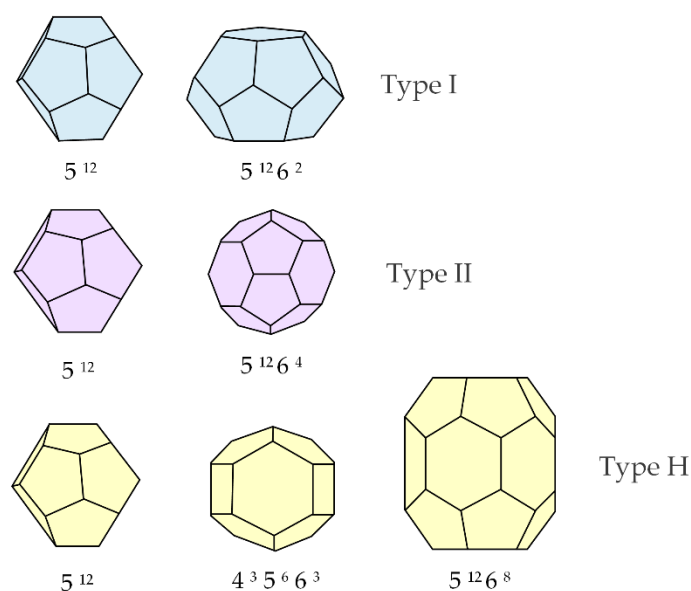


**Figure 1.** Different cages of gas hydrates ( $N^m$ , where N—number of angles in a polyhedron and m—number of polyhedron faces).

Specific aspects of gas hydrate formation in different media were discussed in References [23,74,80–82]. Zang et al. [82] showed that there are two periods in gas hydrate formation. During the first period, gas hydrate emerges at the gas–sediment interface. In the second period, a hydrate of methane is formed in the bulk of sediments. Such behavior of gas hydrates is typical of thin sediments (150–250  $\mu\text{m}$  and 250–380  $\mu\text{m}$ ) [82]. The formation of gas hydrates associated with cold seeps was detected at many locations, such as at the seafloor of the South China Sea [83] and in sedimentary basins of Brazil [27] and New Zealand [84]. Guo et al. [24] found that the initial hydrate formation can proceed throughout sedimentary matrices as a result of a substantial contact of gas with water in the gas flow. In particular, the appreciable quantity of heat released from the formation of gas hydrate can even locally cause neighboring hydrates to dissociate. Hydrates formed faster under higher formation pressures and flow rates of gas. This confirms the decisive sufficient gas–water contact role in the formation of gas hydrate. Still, a great amount of residual water remains right to the end of the formation process [24].

During hydrate formation, the slow kinetics and stochastic induction time determine the inevitable use of hydrates when storing energy in large-scale applications. Surface-

active materials have been applied since the 1990s to improve the methane hydrate formation kinetics [85,86]. Additionally, amino acids enhance the kinetics of hydrate formation. Amino acids are believed [87,88] to facilitate methane hydrate formation, which indicates that they can accumulate methane in hydrates. The morphology studies of gas hydrate formation in the presence of an amino acids under normal conditions identified a “breathing” effect [89], in addition to the formation of methane bubbles in the solution volume. The emerging methane hydrates were flexible enough to allow the methane bubble to expand deep inside the water solution, thus contributing to hydrate growth in a plain, motionless configuration. Another benefit of an amino acid is the absence of foaming during gas extraction, unlike it is with kinetic activators based on surfactants [87]. Veluswamy et al. [88] proposed a hybrid combinatorial approach to methane hydrate formation, using the beneficial aspect of an environmentally friendly amino acid (leucine) as a kinetic promoter. This simple hybrid approach can be easily implemented and extended to develop an economical technology for the efficient large-scale storage of natural gas. An additional benefit of such a method is that little energy is consumed during hydrate growth, which reduces the overall costs of natural gas storage. Okutani et al. [90] showed the results of the experimental study on the effect of adding surfactants (sodium dodecyl sulfate, sodium tetradecyl sulfate, and sodium hexadecyl sulfate) on the characteristics of gas hydrate formation. These surfactants qualitatively change hydrate formation in the same way. The water saturation and the grain size of quartz sand affect hydrate formation kinetics [91]. The experimental data on gas hydrate nucleation and growth in the presence of water-soluble polymer, nonionic surfactants, and their mixtures were presented by Semenov et al. [92].

At present, the patterns of dissociation are well-understood mainly for gas hydrates with the unit cell *sI*. Gas hydrate dissociation (decomposition into gas and water) is a phase transition accompanied by a set of complex physical and chemical processes developing with the absorption of a great amount of heat [28]. There are substantial differences in the decomposition of gas hydrates at above-zero temperatures and their dissociation at temperatures below the freezing point [28]. At positive temperatures, gas diffusion occurs through a water film or layer [93]. Since gas hydrate dissociation is accompanied by cooling, heat exchange with the environment should be taken into account [94]. The effect of heat transfer from the environment on the mechanism of gas hydrate breakup was investigated in References [95–97]. The rates of gas hydrate formation and decomposition are limited by the thermal delay of the environment and the diffusion of gas in a liquid and solid body. Thus, gas hydrate dissociation should take account of the kinetics and heat exchange. At temperatures below 0 °C, the physics of gas hydrate decomposition are more complex due to the emergence of different ice structures and surface morphology. A review of the formation and dissociation of methane gas hydrates was presented by Malagar et al. [31]. A critical synthesis revealed that, for the laboratory modeling of natural gas hydrate habitats, it is important to take into consideration not only the temperature (thermodynamic) conditions, sediments, and their matrix characteristics but also the diameters of sediments, initial water, saturation, density, salinity, mineralogy, and sample volume. The effect of pore diameter and salinity on the thermodynamic equilibrium conditions was also highlighted. These conditions affect hydrate saturation. Gas hydrate formation was shown [98] to depend on the specific area of sediments. Takeya [98] noted that the initial water saturation determines the hydrate habitat type, and there is an optimal value of these thermodynamic conditions and sediment matrix characteristics to achieve the maximum hydrate saturation.

Gas hydrate dissociation is determined by the following key factors [99]: the degree of temperature and pressure deviation from the equilibrium curves, particle-size distribution, average diameter of hydrate granules, and the strength and structural characteristics of the ice crust.

At negative temperatures, a self-preservation effect emerges in hydrate dissociation [100]. With a temperature rise from 230 K to 268 K, the dissociation rate decreases severalfold. This region of annealing is referred to as self-preservation [99]. The self-preservation effect

of gas hydrates was discovered experimentally by Yershov et al. [101]. Later, Yakushev and Chuvilin [102] examined the process of gas hydrate self-preservation in sediments. Self-preserving gas hydrates can be located throughout the permafrost section without favorable thermodynamic conditions [102]. The self-preservation characteristics and mechanism are affected by the hydrate layer thickness and diameter of the hydrate particles [103]. During gas hydrate dissociation, a tight ice envelope is formed on the particle surface. It prevents gas hydrates from fast dissociation. When the temperature approaches the melting point, the fluidity of ice leads to a sharp drop in its tensile strength and a considerable growth in the rate of dissociation [104]. Takeya et al. [98] explored the effect of ice structures on dissociation kinetics. They showed that gas hydrates stored under anomalous preservation conditions are covered with a thin layer of ice and stabilized by it. The thickness of the ice layer was not uniform, with an average thickness of about 100  $\mu\text{m}$  after 24-h storage at 253 K. Takeya [98] found that the inner part of the gas hydrate retained a high storage capacity for methane even after spending a month under unstable conditions. The effect of pressure and temperature on the gas hydrate dissociation rate and the textural changes during dissociation were investigated by Stern et al. [105]. The experiments revealed that the dissociation rate decreased with a higher pressure. It was noted [105] that the gas hydrate self-preservation effect is based on the morphological changes inside the hydrate material but not on the development of an ice crust. Later, Chuvilin et al. [106] studied the dissociation and self-preservation of gas hydrates. They found that methane hydrates can survive for a long time at temperatures from  $-5$  to  $-7$   $^{\circ}\text{C}$  at a pressure below equilibrium, which indicates the effect of self-preservation [106].

The dissociation process of methane hydrate has been studied to understand its stability in the natural environment [107]. Takeya et al. [107] showed that intergranular forces within the pores or granules voids affect the kinetics of methane hydrate dissociation. The evolution of the ice cover of gas hydrate during dissociation in the high-temperature region of an anomalous decomposition was described by Falenty et al. [108]. The powder with larger granules featured a lower dissociation rate. The research findings [109] also revealed that samples with smaller particle sizes were characterized by higher dissociation rates. Misyura [99] showed that the dissociation rate was proportional to the air flow rate, and the dissociation rates corresponded to the range of  $4\text{--}6 \cdot 10^3$   $\text{kg}/(\text{s}^2)$ . With a rise in the airflow rate, the flame approached the hydrate surface and received more heat during dissociation.

Misyura [110] obtained equations to evaluate the effect of several key factors on dissociation during the methane hydrate and double gas hydrates of methane-propane and methane-isopropanol combustion: the dynamic, thermal, and geometric parameters of the working area. The rate of gas hydrate dissociation  $j_D$  and heat flux density  $q$  are given by Equation (1) [110]:

$$j_D \sim (q)^{0.58}. \quad (1)$$

Equation (2) reflects the dependence of the dissociation rate on the key thermal, geometric, and dynamic parameters [110]:

$$j_D \sim (\lambda \Delta T)^{0.58} (V_{ef})^{0.29} (L)^{-0.29} (Pr)^{0.33}, \quad (2)$$

where  $\Delta T$  is the mean difference between the maximum gas temperature in the boundary layer and the average surface temperature of the layer,  $V_{ef}$  is the effective gas rate in the dynamic boundary layer,  $L$  is the length of the site with the hydrate, and  $Pr$  is the Prandtl number.

When describing the gas hydrate dissociation rate, it is important to take into consideration not only the kinetics of dissociation but also the heat and mass transfer inside porous solids [111]. Hassanpouryouzband et al. [112] presented the kinetics of gas hydrate formation and dissociation.

At freezing temperatures (temperatures below the melting ice point) of gas hydrate breakup, the morphology of ice changes greatly. In this case, the porosity decreases signifi-

cantly, and the diffusion coefficient increases, which complicates the breakup modeling. A gas hydrate dissociation diffusion model accounting for the “self-preservation” effect was considered by Vlasov et al. [32,33]. The diffusion–kinetic model of a gas–hydrate film growth was described in Reference [113]. At present, there have been few studies on the modeling of gas hydrate dissociation in a wide range of negative temperatures, since the dissociation rate may decrease by four orders of magnitude when the temperature changes. A simple analytical model of gas hydrate breakup controlling for the dependence of ice film porosity on the temperature was presented by Misyura et al. [29].

Comprehensive studies on gas hydrate dissociation are instrumental in searching for the optimal conditions for gas hydrate production, storage, and combustion. Some issues concerning the dissociation of gas hydrates deep underwater remain unresolved even now. One of the immediate problems is that there are no research findings for the effects of sediments and their matrices on hydrate saturation, as well as on the formation and dissociation rates. Gas hydrate dissociation at negative temperatures remains understudied as well. There are no mathematical or physical models describing the dissociation of gas hydrates under different conditions.

### 3.2. Exploration, Extraction, and Transportation

Gas hydrates are a hard-to-reach energy resource, as about 98% of deposits occur at a water depth of more than 200–700 m, and 2% are in the polar regions. Therefore, problems associated with the industrial production of gas hydrates and their transportation from extraction sites come up already at the stage of developing the deposits [30]. Boswell et al. [114] outlined an approach to conventional prospecting for gas hydrates. It was developed and tested through a series of successful marine exploration programs.

There are currently several methods of detecting gas hydrate deposits: seismic surveys [115–117], measurements of thermal and diffusion flows under a deposit, and electromagnetic field dynamics investigation in the region under study [43].

When gas hydrates are detected with the electromagnetic field, one elongated dipole of the transmitter is used [43]. It either trails on the seafloor or moves like a system of deep-water transmitters several dozens of meters above the seafloor. Duan et al. [43] developed a new transmitter system, Sputnik, which is placed on the seafloor and excites dual perpendicular horizontal polarization of the transmitter at each transmitting station. The transmitted signals are measured with remote stationary receivers fixed on the seafloor.

A multichannel seismic survey [116] was carried out using the high-resolution deep-towed acoustics/geophysics system (DTAGS) to image the structure of deep-sea gas hydrates and to determine the velocity profile of the hydrated sediments. Currently, a new gas hydrate tracking method is being used with a stepwise seismic inversion and 3D seismic datasets with two different resolutions [117]. Then, the obtained high-resolution acoustic impedance is used to trace thin layers that cannot be harnessed with conventional methods [117].

The main challenge is to extract the methane (as free gas) from the hydrate cage, which is usually done via dissociation. Methane hydrates decompose into water and gas when heated or at a falling pressure (conditions necessary for lifting it from the seafloor). There are three main methods of producing gas from gas hydrates (Figure 2). One of the methods involves reducing the pressure and pumping in inhibitors into the reservoir [41,42,118–120]. Another method (thermal) provides a gas inflow from the hydrate formation as a result of a temperature increase [121,122]. The third method combines reducing the pressure with a simultaneous heat supply to the well [123,124] and is considered the most promising. Combined methods involve the decomposition of hydrates accompanied by a pressure reduction with simultaneous thermal impact. Depressurization will make it possible to save the thermal energy input into hydrate dissociation, whereas the heating of the boundary environment will prevent the repeated formation of gas hydrates in the reservoir [123,124]. One important drawback of all the known methods is the high cost of gas production.

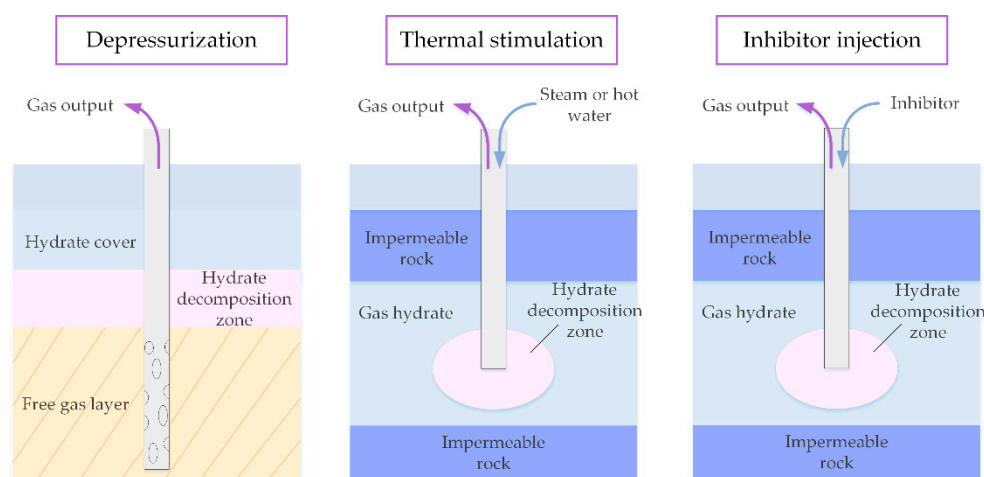


**Figure 2.** Main methods of gas production from gas hydrates.

During depressurization [41,42,118–120], when the operating pressure falls below the equilibrium pressure, the ambient heat is absorbed to dissociate hydrates into gas and water [97]. The production of gas during the depressurization of methane hydrate reservoirs can be divided into three stages (free gas, mixed gas, and gas from dissociated methane hydrate) [125]. During depressurization, no artificial heat is supplied. Thus, the depressurization method is more efficient than a thermal stimulation [121,122]. Still, depressurization does not last long. After the operating pressure is reduced below the preset value, the pressure is not lowered anymore. Hydrates dissociate under ambient heat [126]. This leaves a lot of hydrates in reservoirs. A sustainable gas hydrate production cannot be achieved by reducing the pressure. The advantages of this method include a relatively low cost, a possibility of obtaining large volumes within a short time, and the ease of gas extraction. Its drawback is that the water released during depressurization at low temperatures may freeze and block up the equipment [121,122].

An inhibitor injection is regarded as a way to upset the equilibrium of a gas hydrate and reduce its temperature. Organic solutions (ethanol, methanol, and others) and brine can be used as inhibitors [127]. Controlling the volume of gas extraction by varying the injected inhibitor volume and the prevention of water freezing are the benefits of this method. The drawbacks include high costs and slowly proceeding chemical reactions of the inhibitor with the gas hydrate, as well as the environmental hazard (chemicals leakage on the ocean floor) [44].

Several studies were conducted to investigate natural gas production from gas hydrates by using decompression and thermal stimulation [45,128]. Chen et al. [45] showed that the thermal stimulation method (hot water injection) yields gaseous methane at a rate of  $\sim 10^2$  m<sup>3</sup>/d, whereas depressurization methods may produce one or two orders of magnitude higher values. Such developments demonstrate a real possibility of the industrial application of gas hydrates in the near future, despite numerous problems that should be solved to accomplish commercial purposes [128]. The benefits of thermal stimulation are its ease and lack of sophisticated equipment. The major problems identified during test extractions are associated with increased performance and the difficulty of long-term continuous operation [129]. The first problem requires an in-depth study of the dissociation and dynamics of a multiphase flow under the complex layers bearing gas hydrates underneath the seafloor. The second problem calls for upgrading the current technologies and hardware [128].

A combination of depressurization and thermal stimulation produces a synergistic effect and improves the efficiency of extraction when developing hydrate deposits [46]. Heat is introduced by injecting hot water, steam, using microwaves, or electrical heating [47,48,50]. Hot water or steam injection is of interest to researchers. As pointed out by Song et al. [97], in terms of the energy efficiency and gas production rate, the combined method has obvious



advantages over those utilizing a single procedure. Feng et al. [123] noted that hot water injection enhanced thermal convection. The combined method also reduces the secondary hydrate formation [49].

One important area in scientific and development studies on gas hydrates is related to transportation and storage challenges. Since the 1940s, gas hydrates have been considered an attractive alternative for natural gas transportation and storage [51]. On the one hand, a hydrate of methane is produced and stored under milder conditions (e.g., it is formed at 275.15 K, 3.2 MPa and stored at a temperature of  $-150\text{ }^{\circ}\text{C}$  in the normal atmosphere), whereas compressed natural gas requires a high pressure (20 MPa), and liquefied natural gas requires a low temperature ( $-160\text{ }^{\circ}\text{C}$ ) [130]. On the other hand, hydrate dissociation is a rather slow process that also requires heat, which helps to reduce the risk of gas explosion or leaks [131].

Artificially synthesized hydrates have become high-potential media for natural gas storage due to several benefits [88]. Storing natural gas in clathrate hydrates or solidified natural gas is safe, clean, and compact, which is aided by the relative ease of natural gas extraction with minimal costs as compared with the known conventional storage methods [88]. Practical strategies of commercializing gas hydrates as a medium for natural gas transportation and storage were explored by Song and Mimachi et al. [132,133]. The modeling of gas production from gas hydrate deposits should take into consideration the porosity and heat exchange in porous sediments. A gas hydrate of numerical investigation deposits in deep frozen soil was presented by Musakaev et al. [52]. Gas hydrate deposits can be used for carbon dioxide sequestration as a way to deal with environmental problems [53,54]. The problems of gas replacement and  $\text{CO}_2$  sequestration were studied by Lee et al. [134]. The progress of technologies of hydrate-based  $\text{CO}_2$  capture and separation from mixed gas was considered by Xu et al. [135].

Gas hydrate production has its downsides, though. It may contribute to climate change and global warming, endanger the flora and fauna, harm human health and life, and be a global threat to the environment on the whole [55].

Upgrading and improving the existing technologies for easier and cheaper production of gas hydrates and extraction of natural gas from them remains a relevant issue. It is also important to identify or estimate the saturation of potential gas hydrate deposits within the stability zone.

### 3.3. Combustion Behavior of Gas Hydrate

Gas hydrate combustion is an interesting phenomenon in terms of energy applications and environmental safety [56]. The process poses the combustion of the solid hydrate, not methane from dissociated hydrate (which is simply natural gas). Most research programs aiming at exploiting potential methane hydrate resources focus on the extraction of methane gas and then transporting this natural gas in pipelines just as any other natural gas. The potential technological problems associated with combustion include using hydrates as heat sources for the additional dilution of hydrates, safety during gas storage, and low-emission energy, since hydrates are a only fuel that is quite diluted (considering the content of water) [56]. Scientific research into the ignition of gas hydrates and demonstrations of their potential benefits are quite limited [57,62,66,72,95], yet hydrates, in general, are extensively studied in chemistry and resource surveys of natural hydrates (e.g., References [136,137]). Gas hydrates ignition and combustion are accompanied by numerous phase transformations, which adds new perspectives on the research in the physics and chemistry of combustion [46]. However, due to the special methane hydrates composition, their combustion differs from that of normal liquid or solid fuel in that hydrates of methane undergo complex heterogeneous combustion [56]. The whole process involves the dissociation of hydrate, formation of liquid water and methane bubbles, diffusion flame of methane/air/steam, ice formation, and water evaporation. Hydrate combustion looks somewhat like devolatilization followed by the combustion of volatiles during coal combustion [56,138]. In the first phase of coal combustion, volatile hydrocarbons are released from

the coal particle under thermal impact. This leaves minerals and carbon-rich char. In the same way, hydrate thermal dissociation extricates volatile methane and leaves behind water. On both occasions, the volatile combustible gas burns and produces the heat necessary to continue the process. The difference is that the carboniferous is also combustible, while the residual water from hydrates is not. Nonetheless, continuous hydrate combustion necessitates providing energy to release a sufficient amount of volatiles, which contribute enough energy to maintain the flammable gas subsequent release during combustion.

Chien and Dunn-Rankin [56] described two important aspects of methane hydrate combustion—ignition and stable combustion. A sample of hydrate was ignited with a butane flame lighter and a piezo ignitor. The hydrate flame spectrum was studied using a Princeton Instruments SpectraPro 2300i with a PIXIS 400 detector. The images of the flame were recorded with a standard digital single-lens reflex (DSLR) camera. The findings [56] indicated that the sample should reach some minimum temperature for stable combustion. This temperature was varied depending on the hydrate sample shape. Cylindrical hydrate samples burned steadily at a temperature of  $-25\text{ }^{\circ}\text{C}$  in the center [52], whereas according to Reference [56], the temperature had to be at least  $-4\text{ }^{\circ}\text{C}$ . The reason for the lower temperature is that sufficient heat is required from the flame to increase the temperature of the hydrate to dissociate at a rate sufficient to sustain the heat release needed for further dissociation. The comparison of combustion caused by different heating sources allows raising the gas hydrate combustion efficiency. Practical applications use different schemes of heat supply to initiate combustion, in which conductive, convective, or radiant heat exchange usually dominate or there is a mixed heat exchange [58] (Figure 3). An experimental study into the combustion of double (propane–methane) hydrate samples was conducted by Misyura et al. [59] using different heating schemes. Those included conductive, radiant, and convective heating, local heating by a hot particle, as well as heating in the absence of forced gas flow. The minimum temperature of combustion initiation of the double hydrate corresponds to combustion under the conditions of radiant heating. The maximum dissociation rate of gas hydrates is achieved using induction heating [59].

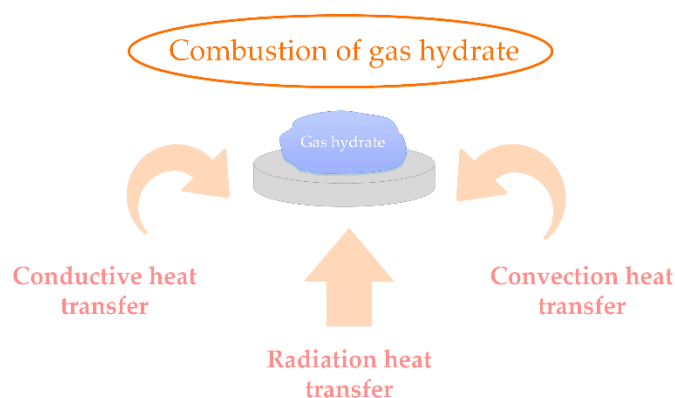


**Figure 3.** Scheme of the heat supply for gas hydrate combustion initiation.

To estimate the effect of gas hydrate geometry on the ignition characteristics, researchers have experimentally studied the combustion behavior of powder [56,58,111], cylindrical [66], and spherical [62,63,69,70] hydrate forms. Their findings revealed that gas hydrates in powder form are ignited more easily and burn out more completely. On the contrary, massive, cylindrical, and spherical hydrates feature unstable combustion.

It is important to explore the behavior of methane hydrate flame to evaluate the energy efficiency of methane hydrate direct combustion [63]. In Reference [63], the flame was generated by ascending flow due to natural convection. The processes during gas hydrate combustion were recorded by a high-speed video camera. The flame temperature is closely connected with the characteristics of flame heat transfer and is used as an important parameter for the evaluation of methane hydrate energy efficiency as a fuel [63].

Wang et al. [63] experimentally studied the combustion flame behavior of methane hydrate spheres, as well as the effect of the sphere diameter and initial temperature in the center on the characteristics of flame. Four stages of gas hydrate combustion were distinguished: stage (I) is combustion development (the flame height increases gradually), stage (II) is rapid combustion (the flame height remains at a high level), stage (III) is stable combustion (the flame height is gradually decreasing), and stage (IV) is fading (the flame height is kept low) [63] (Figure 4).

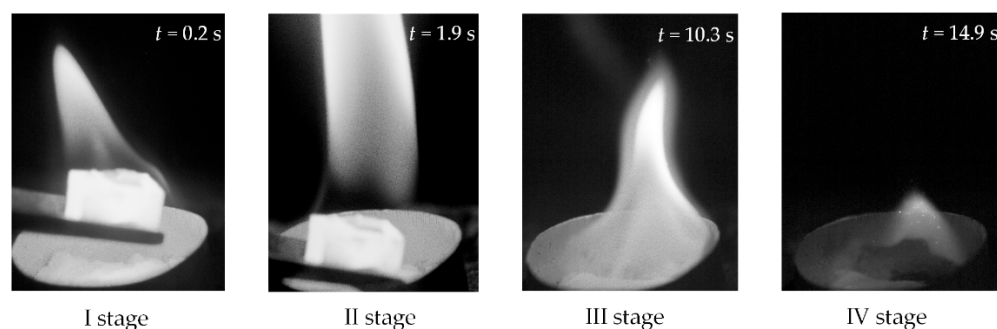


**Figure 4.** The main stages of gas hydrate combustion (local heating by a hot metal particle).

The hydrate sphere diameter has a significant effect on the burning characteristic. As the sphere diameter increases, the flame goes up sharply, and the oscillation frequency decreases, whereas the maximum flame temperature remains constant. Flame parameters such as oscillation characteristics, morphology, and temperature are traditionally considered important in the fundamental research into combustion [139]. The spectral measurements show [56] that the proportion of total flame brightness remains almost constant throughout combustion, i.e., the flame color does not change significantly over time. The overall intensity changes as the flame wavers around the hydrate source. The floating stream produced by the rising hot gases wavers too, which lends dynamic behavior to the flame. However, the opposite was found by Cui et al. [70]: the flame of methane hydrate spheres with a high gas content was bright yellow, whereas that with a low gas content was pale blue. In the case of spherical hydrate combustion [62], the flame fluctuation is caused by the growing surface of the water. The falling water droplets cut off the point where flame is fixed and create fluctuations. Yoshioka et al. [62] established that methane hydrate sphere combustion comprises two stages. At the start of the combustion, the temperature of the surface is lower than the freezing point of water, while the hydrate surface is dry (the first stage). In several seconds, the surface temperature exceeds the freezing point, and water emerges (the second stage). In their experiments, Chien et al. [56] also demonstrated the effects caused by the influence of water, though not with a constant frequency. The flame kept changing around the fuel sample. It was shown [70] that, during a direct massive methane release or direct combustion of supercooled hydrate at atmospheric pressure, a layer of ice or water is formed on the methane hydrate surface. It decreases the surface porosity, thus preventing further methane release. This phenomenon is referred to as self-preservation [60]. Cui et al. [71] investigated the combustion of methane hydrate under the conditions of natural convection, external horizontal air flow, and internal vertical air flow. They analyzed the effects of different air flow shapes on methane hydrate combustion. Their findings [71] revealed that natural convection and horizontal air flow brought about an “eruption phenomenon” destroying the gas hydrate ice layer. A great amount of methane gas escaped instantly, producing a high, bright flame. Under the horizontal airflow conditions, the tilted flame increased the heat transfer to the gas hydrate surface. The flame tilt angle at the rapid combustion stage were smaller than during the steady combustion stage ( $61.26^\circ$  vs.  $70.85^\circ$ ) [71]. Misyura et al. [99] recorded a “mushroom-like” flame during combustion of a methane hydrate. Its formation was explained by the fact that the concentration of gaseous methane in the bubble was too high for it to burn out fast, and it continued burning at a distance from the wall, where there were rather high oxygen

concentrations. A lot of methane combustion elementary reactions are chain termination reactions requiring high activation energy and temperatures. Consequently, the flame has to be maintained at a high temperature, while the temperature near the hydrate surface is low, which leads to dark zone formation. The presence of the latter reduces not only the heat transfer rate from the combustion flame to the hydrate but also the flame stability [140].

Currently, numerical modeling methods are commonly used to analyze flame behavior during the combustion of methane hydrate. Bar-Kohany et al. [64] proposed a model involving an intermediate layer of the bubble mixture when describing the combustion of methane hydrate and allowing for particles with the initial radius of 100  $\mu\text{m}$  or less to clarify the self-preservation effect. A mathematic model to identify a mass release with the self-preservation phenomenon is complicated [65]. The modeling of gas hydrate combustion at negative sample temperatures has such interrelated problems as the unsteady non-isothermal nature of gas hydrates combustion and dissociation, the formation of a water film, the formation of cracks in the hydrate layer, a water evaporation simultaneous effect, inhomogeneous and unsteady combustion, and the influence of the natural convection of gas on the gas hydrate breakup rate [61]. Interrelated heat transfer processes were numerically studied for methane hydrate ignition in the course of conductive heating at negative sample temperatures [58]. It was established [58] that an increase in the heater surface temperature from 973 to 1273 K reduced the ignition delay times of methane hydrate almost tenfold. Moreover, there have been some experimental and numerical study results for the behavior of flames spread over clean methane hydrate in the laminar boundary layer [141,142]. Wu et al. [65] showed that methane hydrate combustion in porous burners provides a steady homogeneous flame, which makes it possible to explore the heat and mass transfer mechanisms that are crucial for studying methane hydrate release. The variational characteristics of a flame during the combustion of methane hydrate (2.7 cm in diameter) was experimentally studied by Cui et al. [67]. The effect of water on the behavior of a methane hydrate combustion flame was also investigated, and the amount of evaporating water during the combustion was measured. The way water steam affects the combustion reaction was explored using a chemical dynamics simulation [67]. The research findings [67] explained the mechanism of water impact on the flame during the combustion of methane hydrate at the microscopic and macroscopic levels, which is of great practical importance for engineering. For instance, in terms of storage and transportation technologies relying on safety improvement, using meltwater is considered for automatic flame quenching during accidental fires. With economic considerations and energy efficiency in mind, a conclusion was made that fast drainage is required to provide the most complete burnout of gas hydrates [67]. The heat and mass transfer effect on the hydrate decomposition rate when considerably varying the heat flux was studied by Nakoryakov et al. [57]. It was shown that the hydrate dissociation rate during combustion was severalfold higher than that of natural dissociation. The dissociation rate depends greatly on the heat flux and diffusion rate [57]. The modeling of the combustion flame behavior of water vapor-laden methane without convective stream premixing showed [143] that the maximum flame temperature decreased with an increase in the content of water, whereas the limit of the water content in gas increased with a lower shear rate. The research findings for methane hydrate combustion in an opposed-jet porous burner were presented by Wu et al. [65]. The measured flame temperature was about 1700 K. The diffusion flame of methane hydrate was modeled by means of GRI MECH 3.0. The modeling of gas hydrate dissociation should factor in the heat flux, diffusion processes, and particle sizes [144]. Xenon and nitrous oxide-containing hydrates were modeled by Bozhko et al. [145]. The modeling of methane hydrate combustion controlling for water steam formation was performed by Bar-Kohany et al. [64,68]. The estimated maximum steam concentration at the surface of the spherical particle of the above-mentioned authors was 0.6, whereas the maximum flame temperature corresponded to the range of 1700–1750 K. In gas hydrate layer combustion, the effect of the kinetics of gas hydrate dissociation on combustion kinetics should be taken into consideration. A high heat flux from the combustion region to the layer surface and a

high steam concentration in the flame area significantly reduce the flame temperature. The equations considering both the breakup and combustion of gas hydrates were modeled by Misyura et al. [111].

Combustion dynamics concern not only energy efficiency but also safety issues. Yet, due to the hydrate layer vulnerability, unjustifiable extraction brings about disastrous effects: marine ecosystem destruction, global warming, and geological hazards [146].

Despite recent extensive studies on gas hydrates, there are still a lot of unresolved issues that have to be dealt with to improve the efficiency of technologies during actual practice. There are no models of gas hydrate ignition taking into account the dissociation processes and the self-preservation effect. There is not enough theoretic research to define the ignition characteristics of natural and artificial gas hydrates when varying the key parameters in wide ranges that are promising for industrial applications and which are difficult to provide experimentally due to a high fire and explosion hazard. Another understudied issue is the combustion of gas hydrate all over the sample layer due to its heterogeneity. No comparison has been conducted for the ignition behavior of layered and powdered gas hydrates when varying the different parameters and conditions. In our opinion, the solution to these issues will be the following developments. At present, research on gas hydrates is relevant and undertaken by scientists in all three areas.

#### 4. Conclusions

The energy potential of gas hydrates can provide the world with clean energy. At the same time, developing gas hydrates as a new energy resource requires careful study. Three main research areas on the gas hydrates have been distinguished: formation aspects, technologies of gas hydrate extraction and transportation, and the investigation of ignition and combustion. Our research presents a review of the major studies available today in all of these areas. The main aspects of studying gas hydrates were defined. We presented the most interesting results, dependences, and characteristics obtained for the production processes involving hydrates. Gas hydrates are a complex and multifaceted problem requiring coordinated effort on a global scale.

**Author Contributions:** O.G.—writing, review and editing; S.M.—writing, review and editing and P.S.—writing, review and editing. All authors have read and agreed to the published version of the manuscript.

**Funding:** This research was funded by a grant from the Ministry of Science and Higher Education of Russia, Agreement No. 075-15-2020-806 (Contract No. 13.1902.21.0014).

**Conflicts of Interest:** The authors declare no conflict of interest.

#### Nomenclature

$\Delta T$	average difference between the maximum gas temperature in the boundary layer and the average surface temperature of the layer, K
$V_{ef}$	effective gas rate in the dynamic boundary layer, m/s
$L$	length of the site with hydrate, m
$Pr$	the Prandtl number
$t$	gas hydrate combustion time, s
$j_D$	gas hydrate dissociation rate, m/s
$q$	heat flux density, W/m <sup>2</sup>
$\lambda$	thermal conductivity, W/(m·K)

#### References

1. Liu, C.; Ye, Y. *Natural Gas Hydrates: Experimental Techniques and Their Applications*; Springer: Berlin/Heidelberg, Germany, 2013; ISBN 9783642311017.
2. Gao, Q.; Yin, Z.; Zhao, J.; Yang, D.; Linga, P. Tuning the fluid production behaviour of hydrate-bearing sediments by multi-stage depressurization. *Chem. Eng. J.* **2021**, *406*, 127174. [[CrossRef](#)]
3. Sloan, E.D. Fundamental principles and applications of natural gas hydrates. *Nature* **2003**, *426*, 353–359. [[CrossRef](#)]

4. Klauda, J.B.; Sandler, S.I. Global distribution of methane hydrate in ocean sediment. *Energy Fuels* **2005**, *19*, 459–470. [[CrossRef](#)]
5. Zhou, S.; Li, Q.; Lv, X.; Fu, Q.; Zhu, J. Key issues in development of offshore natural gas hydrate. *Front. Energy* **2020**, *14*, 433–442. [[CrossRef](#)]
6. Boswell, R.; Collett, T.S. Current perspectives on gas hydrate resources. *Energy Environ. Sci.* **2011**, *4*, 1206–1215. [[CrossRef](#)]
7. Istomin, V.A.; Yakushev, V.S. *Gas Hydrates in Nature*; Nedra: Moscow, Russia, 1992.
8. Liu, L.; Ryu, B.J.; Sun, Z.; Wu, N.; Cao, H.; Geng, W.; Zhang, X.; Jia, Y.; Xu, C.; Guo, L.; et al. Monitoring and research on environmental impacts related to marine natural gas hydrates: Review and future perspective. *J. Nat. Gas Sci. Eng.* **2019**, *65*, 82–107. [[CrossRef](#)]
9. Rui, Z.; Wang, X. A comprehensive analysis of natural gas distribution pipeline incidents. *Int. J. Oil Gas Coal Technol.* **2013**, *6*, 528–548. [[CrossRef](#)]
10. Sohn, Y.H.; Kim, J.; Shin, K.; Chang, D.; Seo, Y.; Aman, Z.M.; May, E.F. Hydrate plug formation risk with varying watercut and inhibitor concentrations. *Chem. Eng. Sci.* **2015**, *126*, 711–718. [[CrossRef](#)]
11. Misyura, S.Y. Comparing the dissociation kinetics of various gas hydrates during combustion: Assessment of key factors to improve combustion efficiency. *Appl. Energy* **2020**, *270*, 115042. [[CrossRef](#)]
12. Kozhevnykov, A.; Khomenko, V.; Liu, B.; Kamyshatskyi, O.; Pashchenko, O. The history of gas hydrates studies: From laboratory curiosity to a new fuel alternative. *Key Eng. Mater.* **2020**, *844*, 49–64. [[CrossRef](#)]
13. Collett, I.S.; Ehlig-Economides, C.A. Detection and evaluation of the in-situ natural gas hydrates in the north slope region, Alaska. In Proceedings of the SPE California Regional Meeting, Ventura, CA, USA, 23–25 March 1983; pp. 97–106. [[CrossRef](#)]
14. Collett, T.S.; Bird, K.J.; Kvenvolden, K.A.; Magoon, L.B. The origin of natural gas hydrates on the north slope of Alaska. *US Geol. Surv. Bull.* **1989**, *1903*, 3–9.
15. Collett, T.S. Natural gas hydrates of the Prudhoe Bay and Kuparuk River area, North Slope, Alaska. *Am. Assoc. Pet. Geol. Bull.* **1993**, *77*, 793–812. [[CrossRef](#)]
16. Shipley, T.H. Seismic evidence for widespread possible gas hydrate horizons on continental slopes and rises. *Am. Assoc. Pet. Geol. Bull.* **1979**, *63*, 2204–2213. [[CrossRef](#)]
17. Brooks, J.M.; Kennicutt, M.C.; Fay, R.R.; McDonald, T.J.; Sassen, R. Thermogenic gas hydrates in the Gulf of Mexico. *Science* **1984**, *225*, 409–411. [[CrossRef](#)]
18. Murota, T. Gas hydrate exploration: Its technology-environment interface in the World and Japan. *Hitotsubashi J. Econ.* **1996**, *37*, 21–44.
19. Aoki, Y.; Shimizu, S.; Yamane, T.; Tanaka, T.; Nakayama, K.; Hayashi, T.; Okuda, Y. Methane hydrate accumulation along the western Nankai Trough. *Ann. N. Y. Acad. Sci.* **2000**, *912*, 136–145. [[CrossRef](#)]
20. Sum, A.K.; Koh, C.A.; Sloan, E.D. Clathrate hydrates: From laboratory science to engineering practice. *Ind. Eng. Chem. Res.* **2009**, *48*, 7457–7465. [[CrossRef](#)]
21. Koshurnikov, A.V. The Principles of Complex Geocryological Geophysical Analysis for Studying Permafrost and Gas Hydrates on the Arctic Shelf of Russia. *Mosc. Univ. Geol. Bull.* **2020**, *75*, 425–434. [[CrossRef](#)]
22. Wang, Y.; Feng, J.C.; Li, X.S.; Zhang, Y.; Chen, Z.Y. Fluid flow mechanisms and heat transfer characteristics of gas recovery from gas-saturated and water-saturated hydrate reservoirs. *Int. J. Heat Mass Transf.* **2018**, *118*, 1115–1127. [[CrossRef](#)]
23. Li, X.Y.; Feng, J.C.; Li, X.S.; Wang, Y.; Hu, H.Q. Experimental study of methane hydrate formation and decomposition in the porous medium with different thermal conductivities and grain sizes. *Appl. Energy* **2022**, *305*, 117852. [[CrossRef](#)]
24. Guo, X.; Shi, K.; Guan, D.; Lv, X.; Li, Q.; Dong, H.; Zhao, J.; Yang, L.; Liu, Z. Behaviors of CH<sub>4</sub> hydrate formation in cold seeps with underlying gas plume. *Fuel* **2021**, *304*, 121364. [[CrossRef](#)]
25. Jang, J.; Waite, W.F.; Stern, L.A.; Collett, T.S.; Kumar, P. Physical property characteristics of gas hydrate-bearing reservoir and associated seal sediments collected during NGHP-02 in the Krishna-Godavari Basin, in the offshore of India. *Mar. Pet. Geol.* **2019**, *108*, 249–271. [[CrossRef](#)]
26. Gambelli, A.M.; Rossi, F. Thermodynamic and kinetic characterization of methane hydrate ‘nucleation, growth and dissociation processes, according to the labile Cluster theory. *Chem. Eng. J.* **2021**, *425*, 130706. [[CrossRef](#)]
27. Ketzer, M.; Praeg, D.; Pivel, M.A.G.; Augustin, A.H.; Rodrigues, L.F.; Viana, A.R.; Cupertino, J.A. Gas Seeps at the Edge of the Gas Hydrate Stability Zone on Brazil’s Continental Margin. *Geoscience* **2019**, *9*, 193. [[CrossRef](#)]
28. Misyura, S.Y. The influence of porosity and structural parameters on different kinds of gas hydrate dissociation. *Sci. Rep.* **2016**, *6*, 30324. [[CrossRef](#)]
29. Misyura, S.Y.; Donskoy, I.G.; Manakov, A.Y.; Morozov, V.S.; Strizhak, P.A.; Skiba, S.S.; Sagidullin, A.K. Studying the influence of key parameters on the methane hydrate dissociation in order to improve the storage efficiency. *J. Energy Storage* **2021**, *44*, 103288. [[CrossRef](#)]
30. Yu, H.; Xu, T.; Xin, X.; Yuan, Y.; Feng, G.; Chen, Q.; Yu, Z. Optimization of Gas Production from Marine Methane Hydrate Deposit Induced by Horizontal Well. *Energy Fuels* **2021**, *35*, 2531–2544. [[CrossRef](#)]
31. Malagar, B.R.C.; Lijith, K.P.; Singh, D.N. Formation & dissociation of methane gas hydrates in sediments: A critical review. *J. Nat. Gas Sci. Eng.* **2019**, *65*, 168–184.
32. Vlasov, V.A. Diffusion model of gas hydrate dissociation into ice and gas: Simulation of the self-preservation effect. *Int. J. Heat Mass Transf.* **2016**, *102*, 631–636. [[CrossRef](#)]

33. Vlasov, V.A. Diffusion model of gas hydrate dissociation into ice and gas that takes into account the ice microstructure. *Chem. Eng. Sci.* **2020**, *215*, 115443. [[CrossRef](#)]
34. Clennell, M.B.; Hovland, M.; Booth, J.S.; Henry, P.; Winters, W.J. Formation of natural gas hydrates in marine sediments 1. Conceptual model of gas hydrate growth conditioned by host sediment properties. *J. Geophys. Res. Solid Earth* **1999**, *104*, 22985–23003. [[CrossRef](#)]
35. Genov, G.; Kuhs, W.F.; Staykova, D.K.; Goreschnik, E.; Salamatin, A.N. Experimental studies on the formation of porous gas hydrates. *Am. Mineral.* **2004**, *89*, 1228–1239. [[CrossRef](#)]
36. Kumar, A.; Maini, B.; Bishnoi, P.R.; Clarke, M.; Zatsepina, O.; Srinivasan, S. Experimental determination of permeability in the presence of hydrates and its effect on the dissociation characteristics of gas hydrates in porous media. *J. Pet. Sci. Eng.* **2010**, *70*, 114–122. [[CrossRef](#)]
37. Zhang, B.; Zheng, J.; Yin, Z.; Liu, C.; Wu, Q.; Wu, Q.; Liu, C.; Gao, X.; Zhang, Q. Methane hydrate formation in mixed-size porous media with gas circulation: Effects of sediment properties on gas consumption, hydrate saturation and rate constant. *Fuel* **2018**, *233*, 94–102. [[CrossRef](#)]
38. Zhan, J.; Zhang, P.; Wang, Y.; Wu, Q. Experimental research on methane hydrate formation in porous media based on the low-field NMR technique. *Chem. Eng. Sci.* **2021**, *244*, 116804. [[CrossRef](#)]
39. Teng, Y.; Zhang, D. Comprehensive study and comparison of equilibrium and kinetic models in simulation of hydrate reaction in porous media. *J. Comput. Phys.* **2020**, *404*, 109094. [[CrossRef](#)]
40. Jarrar, Z.A.; Alshibli, K.A.; Al-Raoush, R.I.; Jung, J. 3D measurements of hydrate surface area during hydrate dissociation in porous media using dynamic 3D imaging. *Fuel* **2020**, *265*, 116978. [[CrossRef](#)]
41. Yang, M.; Dong, S.; Zhao, J.; Zheng, J.N.; Liu, Z.; Song, Y. Ice behaviors and heat transfer characteristics during the isothermal production process of methane hydrate reservoirs by depressurization. *Energy* **2021**, *232*, 121030. [[CrossRef](#)]
42. Zhao, J.; Zhu, Z.; Song, Y.; Liu, W.; Zhang, Y.; Wang, D. Analyzing the process of gas production for natural gas hydrate using depressurization. *Appl. Energy* **2015**, *142*, 125–134. [[CrossRef](#)]
43. Duan, S.; Hölz, S.; Dannowski, A.; Schwalenberg, K.; Jegen, M. Study on gas hydrate targets in the Danube Paleo-Delta with a dual polarization controlled-source electromagnetic system. *Mar. Pet. Geol.* **2021**, *134*, 105330. [[CrossRef](#)]
44. Shaibu, R.; Sambo, C.; Guo, B.; Dudun, A. An assessment of methane gas production from natural gas hydrates: Challenges, technology and market outlook. *Adv. Geo-Energy Res.* **2021**, *5*, 318–332. [[CrossRef](#)]
45. Chen, L.; Feng, Y.; Okajima, J.; Komiya, A.; Maruyama, S. Production behavior and numerical analysis for 2017 methane hydrate extraction test of Shenhu, South China Sea. *J. Nat. Gas Sci. Eng.* **2018**, *53*, 55–66. [[CrossRef](#)]
46. Liu, Y.; Hou, J.; Chen, Z.; Su, H.; Zhao, E.; Li, G. A novel natural gas hydrate recovery approach by delivering geothermal energy through dumpflooding. *Energy Convers. Manag.* **2020**, *209*, 112623. [[CrossRef](#)]
47. Liu, Y.; Hou, J.; Chen, Z.; Bai, Y.; Su, H.; Zhao, E.; Li, G. Enhancing hot water flooding in hydrate bearing layers through a novel staged production method. *Energy* **2021**, *217*, 119319. [[CrossRef](#)]
48. Wang, B.; Dong, H.; Fan, Z.; Liu, S.; Lv, X.; Li, Q.; Zhao, J. Numerical analysis of microwave stimulation for enhancing energy recovery from depressurized methane hydrate sediments. *Appl. Energy* **2020**, *262*, 114559. [[CrossRef](#)]
49. Guo, X.; Xu, L.; Wang, B.; Sun, L.; Liu, Y.; Wei, R.; Yang, L.; Zhao, J. Optimized gas and water production from water-saturated hydrate-bearing sediment through step-wise depressurization combined with thermal stimulation. *Appl. Energy* **2020**, *276*, 115438. [[CrossRef](#)]
50. Falser, S.; Uchida, S.; Palmer, A.C.; Soga, K.; Tan, T.S. Increased Gas Production from Hydrates by Combining Depressurization with Heating of the Wellbore. *Energy Fuels* **2012**, *26*, 6259–6267. [[CrossRef](#)]
51. Veluswamy, H.P.; Kumar, A.; Seo, Y.; Lee, J.D.; Linga, P. A review of solidified natural gas (SNG) technology for gas storage via clathrate hydrates. *Appl. Energy* **2018**, *216*, 262–285. [[CrossRef](#)]
52. Musakaev, N.G.; Khasanov, M.K.; Borodin, S.L. The mathematical model of the gas hydrate deposit development in permafrost. *Int. J. Heat Mass Transf.* **2018**, *118*, 455–461. [[CrossRef](#)]
53. Shagapov, V.S.; Khasanov, M.K.; Musakaev, N.G.; Duong, N.H. Theoretical research of the gas hydrate deposits development using the injection of carbon dioxide. *Int. J. Heat Mass Transf.* **2017**, *107*, 347–357. [[CrossRef](#)]
54. Khasanov, M.K.; Rafikova, G.R.; Musakaev, N.G. Mathematical Model of Carbon Dioxide Injection into a Porous Reservoir Saturated with Methane and Its Gas Hydrate. *Energies* **2020**, *13*, 440. [[CrossRef](#)]
55. Yan, D.; Farah, P.D.; Gaskova, I.; Giabardo, C.V. Evaluating China's Environmental Management and Risks Avoidance Policies and Regulations on Offshore Methane Hydrate Extraction. *Sustainability* **2020**, *12*, 5331. [[CrossRef](#)]
56. Chien, Y.C.; Dunn-Rankin, D. Combustion characteristics of methane hydrate flames. *Energies* **2019**, *12*, 1939. [[CrossRef](#)]
57. Nakoryakov, V.E.; Misyura, S.Y.; Elistratov, S.L.; Manakov, A.Y.; Shubnikov, A.E. Combustion of methane hydrates. *J. Eng. Thermophys.* **2013**, *22*, 87–92. [[CrossRef](#)]
58. Gaydukova, O.S.; Misyura, S.Y.; Strizhak, P.A. Investigating regularities of gas hydrate ignition on a heated surface: Experiments and modelling. *Combust. Flame* **2021**, *228*, 78–88. [[CrossRef](#)]
59. Misyura, S.Y.; Manakov, A.Y.; Nyashina, G.S.; Gaidukova, O.S.; Morozov, V.S.; Skiba, S.S. Gas hydrate combustion in five method of combustion organization. *Entropy* **2020**, *22*, 710. [[CrossRef](#)]
60. Misyura, S.Y.; Nakoryakov, V.E. Nonstationary combustion of methane with gas hydrate dissociation. *Energy Fuels* **2013**, *27*, 7089–7097. [[CrossRef](#)]

61. Misyura, S.Y.; Morozov, V.S. Influence of Air Velocity on Non-Isothermal Decay and Combustion of Gas Hydrate. *J. Eng. Thermophys.* **2021**, *30*, 374–382. [[CrossRef](#)]
62. Yoshioka, T.; Yamamoto, Y.; Yokomori, T.; Ohmura, R.; Ueda, T. Experimental study on combustion of a methane hydrate sphere. *Exp. Fluids* **2015**, *56*, 192. [[CrossRef](#)]
63. Wang, S.; Cui, G.; Bi, H.; Liu, C.; Dong, Z.; Xing, X.; Li, Z.; Liu, J. Effect analysis on flame characteristics in the combustion of methane hydrate spheres under natural convective flow conditions. *J. Nat. Gas Sci. Eng.* **2020**, *83*, 103578. [[CrossRef](#)]
64. Bar-Kohany, T.; Sirignano, W.A. Transient combustion of a methane-hydrate sphere. *Combust. Flame* **2016**, *163*, 284–300. [[CrossRef](#)]
65. Wu, F.H.; Padilla, R.E.; Dunn-Rankin, D.; Chen, G.B.; Chao, Y.C. Thermal structure of methane hydrate fueled flames. *Proc. Combust. Inst.* **2017**, *36*, 4391–4398. [[CrossRef](#)]
66. Roshandell, M.; Santacana-Vall, J.; Karnani, S.; Botimer, J.; Taborek, P.; Dunn-Rankin, D. Burning Ice—Direct Combustion of Methane Clathrates. *Combust. Sci. Technol.* **2016**, *188*, 2137–2148. [[CrossRef](#)]
67. Cui, G.; Dong, Z.; Wang, S.; Xing, X.; Shan, T.; Li, Z. Effect of the water on the flame characteristics of methane hydrate combustion. *Appl. Energy* **2020**, *259*, 114205. [[CrossRef](#)]
68. Dagan, Y.; Bar-Kohany, T. Flame propagation through three-phase methane-hydrate particles. *Combust. Flame* **2018**, *193*, 25–35. [[CrossRef](#)]
69. Cui, G.; Wang, S.; Dong, Z.; Xing, X.; Shan, T.; Li, Z. Effects of the diameter and the initial center temperature on the combustion characteristics of methane hydrate spheres. *Appl. Energy* **2020**, *257*, 114058. [[CrossRef](#)]
70. Cui, G.; Dong, Z.; Xie, K.; Wang, S.; Guo, T.; Liu, J.; Xing, X.; Li, Z. Effects of gas content and ambient temperature on combustion characteristics of methane hydrate spheres. *J. Nat. Gas Sci. Eng.* **2021**, *88*, 103842. [[CrossRef](#)]
71. Cui, G.; Dong, Z.; Xie, K.; Wang, S.; Guo, T.; Liu, J.; Xing, X.; Li, Z. Experimental study on the effect of airflow conditions on the combustion characteristics of methane hydrate. *Fuel* **2021**, *300*, 120926. [[CrossRef](#)]
72. Wu, F.-H.; Chao, Y.-C. A Study of Methane Hydrate Combustion Phenomenon Using a Cylindrical Porous Burner. *Combust. Sci. Technol.* **2016**, *188*, 1983–2002. [[CrossRef](#)]
73. Chen, B.; Sun, H.; Zhao, G.; Wang, B.; Zhao, Y.; Yang, M. Experimental observation of methane hydrate dissociation via different depressurization modes under water phase flow. *Fuel* **2021**, *283*, 118908. [[CrossRef](#)]
74. Liang, S.; Rozmanov, D.; Kusalik, P.G. Crystal growth simulations of methane hydrates in the presence of silica surfaces. *Phys. Chem. Chem. Phys.* **2011**, *13*, 19856–19864. [[CrossRef](#)] [[PubMed](#)]
75. Yousif, M.H.; Abass, H.H.; Selim, M.S.; Sloan, E.D. Experimental and theoretical investigation of methane-gas-hydrate dissociation in porous media. *SPE Reserv. Eng. Soc. Pet. Eng.* **1991**, *6*, 69–76. [[CrossRef](#)]
76. Yin, Z.; Moridis, G.; Chong, Z.R.; Tan, H.K.; Linga, P. Numerical analysis of experimental studies of methane hydrate dissociation induced by depressurization in a sandy porous medium. *Appl. Energy* **2018**, *230*, 444–459. [[CrossRef](#)]
77. Pauling, L.; Marsh, R.E. The Structure of Chlorine Hydrate. *Proc. Natl. Acad. Sci. USA* **1952**, *38*, 112–118. [[CrossRef](#)] [[PubMed](#)]
78. Claussen, W.F. A Second Water Structure for Inert Gas Hydrates. *J. Chem. Phys.* **2004**, *19*, 1425. [[CrossRef](#)]
79. Ripmeester, J.A.; Tse, J.S.; Ratcliffe, C.I.; Powell, B.M. A new clathrate hydrate structure. *Nature* **1987**, *325*, 135–136. [[CrossRef](#)]
80. Chong, Z.R.; Yang, M.; Khoo, B.C.; Linga, P. Size Effect of Porous Media on Methane Hydrate Formation and Dissociation in an Excess Gas Environment. *Ind. Eng. Chem. Res.* **2015**, *55*, 7981–7991. [[CrossRef](#)]
81. Bhattacharjee, G.; Kumar, A.; Sakpal, T.; Kumar, R. Carbon Dioxide Sequestration: Influence of Porous Media on Hydrate Formation Kinetics. *ACS Sustain. Chem. Eng.* **2015**, *3*, 1205–1214. [[CrossRef](#)]
82. Zang, X.; Liang, D.; Wu, N. Gas hydrate formation in fine sand. *Sci. China Earth Sci.* **2012**, *56*, 549–556. [[CrossRef](#)]
83. Zhang, X.; Du, Z.; Luan, Z.; Wang, X.; Xi, S.; Wang, B.; Li, L.; Lian, C.; Yan, J. In Situ Raman Detection of Gas Hydrates Exposed on the Seafloor of the South China Sea. *Geochem. Geophys. Geosystems* **2017**, *18*, 3700–3713. [[CrossRef](#)]
84. Fraser, D.R.A.; Gorman, A.R.; Pecher, I.A.; Crutchley, G.J.; Henrys, S.A. Gas hydrate accumulations related to focused fluid flow in the Pegasus Basin, southern Hikurangi Margin, New Zealand. *Mar. Pet. Geol.* **2016**, *77*, 399–408. [[CrossRef](#)]
85. Zhong, Y.; Rogers, R.E. Surfactant effects on gas hydrate formation. *Chem. Eng. Sci.* **2000**, *55*, 4175–4187. [[CrossRef](#)]
86. Ganji, H.; Manteghian, M.; Sadaghiani Zadeh, K.; Omidkhah, M.R.; Rahimi Mofrad, H. Effect of different surfactants on methane hydrate formation rate, stability and storage capacity. *Fuel* **2007**, *86*, 434–441. [[CrossRef](#)]
87. Liu, Y.; Chen, B.; Chen, Y.; Zhang, S.; Guo, W.; Cai, Y.; Tan, B.; Wang, W. Methane Storage in a Hydrated Form as Promoted by Leucines for Possible Application to Natural Gas Transportation and Storage. *Energy Technol.* **2015**, *3*, 815–819. [[CrossRef](#)]
88. Veluswamy, H.P.; Kumar, A.; Kumar, R.; Linga, P. An innovative approach to enhance methane hydrate formation kinetics with leucine for energy storage application. *Appl. Energy* **2017**, *188*, 190–199. [[CrossRef](#)]
89. Veluswamy, H.P.; Hong, Q.W.; Linga, P. Morphology Study of Methane Hydrate Formation and Dissociation in the Presence of Amino Acid. *Cryst. Growth Des.* **2016**, *16*, 5932–5945. [[CrossRef](#)]
90. Okutani, K.; Kuwabara, Y.; Mori, Y.H. Surfactant effects on hydrate formation in an unstirred gas/liquid system: An experimental study using methane and sodium alkyl sulfates. *Chem. Eng. Sci.* **2008**, *63*, 183–194. [[CrossRef](#)]
91. Zaripova, Y.; Yarkovoi, V.; Varfolomeev, M.; Kadyrov, R.; Stoporev, A. Influence of Water Saturation, Grain Size of Quartz Sand and Hydrate-Former on the Gas Hydrate Formation. *Energies* **2021**, *14*, 1272. [[CrossRef](#)]
92. Semenov, A.P.; Mendgaziev, R.I.; Stoporev, A.S.; Kuchierskaya, A.A.; Novikov, A.A.; Vinokurov, V.A. Gas hydrate nucleation and growth in the presence of water-soluble polymer, nonionic surfactants, and their mixtures. *J. Nat. Gas Sci. Eng.* **2020**, *82*, 103491. [[CrossRef](#)]



93. Clarke, M.; Bishnoi, P.R. Determination of the intrinsic rate of ethane gas hydrate decomposition. *Chem. Eng. Sci.* **2000**, *55*, 4869–4883. [[CrossRef](#)]
94. Hong, H.; Pooladi-Darvish, M.; Bishnoi, P.R. Analytical modelling of gas production from hydrates in porous media. *J. Can. Pet. Technol.* **2003**, *42*, 45–56. [[CrossRef](#)]
95. Nakoryakov, V.E.; Misyura, S.Y.; Elistratov, S.L.; Manakov, A.Y.; Sizikov, A.A. Methane combustion in hydrate systems: Water-methane and water-methane-isopropanol. *J. Eng. Thermophys.* **2013**, *22*, 169–173. [[CrossRef](#)]
96. Song, Y.; Wang, J.; Liu, Y.; Zhao, J. Analysis of heat transfer influences on gas production from methane hydrates using a combined method. *Int. J. Heat Mass Transf.* **2016**, *92*, 766–773. [[CrossRef](#)]
97. Song, Y.; Cheng, C.; Zhao, J.; Zhu, Z.; Liu, W.; Yang, M.; Xue, K. Evaluation of gas production from methane hydrates using depressurization, thermal stimulation and combined methods. *Appl. Energy* **2015**, *145*, 265–277. [[CrossRef](#)]
98. Takeya, S.; Yoneyama, A.; Ueda, K.; Hyodo, K.; Takeda, T.; Mimachi, H.; Takahashi, M.; Iwasaki, T.; Sano, K.; Yamawaki, H.; et al. Nondestructive imaging of anomalously preserved methane clathrate hydrate by phase contrast x-ray imaging. *J. Phys. Chem. C* **2011**, *115*, 16193–16199. [[CrossRef](#)]
99. Misyura, S.Y. Non-stationary combustion of natural and artificial methane hydrate at heterogeneous dissociation. *Energy* **2019**, *181*, 589–602. [[CrossRef](#)]
100. Xie, Y.; Zheng, T.; Zhong, J.R.; Zhu, Y.J.; Wang, Y.F.; Zhang, Y.; Li, R.; Yuan, Q.; Sun, C.Y.; Chen, G.J. Experimental research on self-preservation effect of methane hydrate in porous sediments. *Appl. Energy* **2020**, *268*, 115008. [[CrossRef](#)]
101. Yershov, E.D.; Lebedenko, Y.P.; Chuvilin, Y.M.; Istomin, V.A.; Yakushev, V.S. The problems of the stability of gas-hydrate deposits in the cryolithozone. *Vestn. Mosk. Univ. Seriya Geol.* **1992**, *5*, 82–87.
102. Yakushev, V.S.; Chuvilin, E.M. Natural gas and gas hydrate accumulations within permafrost in Russia. *Cold Reg. Sci. Technol.* **2000**, *31*, 189–197. [[CrossRef](#)]
103. Prasad, P.S.R.; Chari, V.D. Preservation of methane gas in the form of hydrates: Use of mixed hydrates. *J. Nat. Gas Sci. Eng.* **2015**, *25*, 10–14. [[CrossRef](#)]
104. Takeya, S.; Ripmeester, J.A. Anomalous preservation of CH<sub>4</sub> hydrate and its dependence on the morphology of hexagonal ice. *ChemPhysChem* **2010**, *11*, 70–73. [[CrossRef](#)] [[PubMed](#)]
105. Stern, L.A.; Circone, S.; Kirby, S.H.; Durham, W.B. Temperature, pressure, and compositional effects on anomalous or “self” preservation of gas hydrates. *Can. J. Phys.* **2003**, *81*, 271–283. [[CrossRef](#)]
106. Chuvilin, E.; Bukhanov, B.; Davletshina, D.; Grebenkin, S.; Istomin, V. Dissociation and self-preservation of gas hydrates in permafrost. *Geoscience* **2018**, *8*, 431. [[CrossRef](#)]
107. Takeya, S.; Fujihisa, H.; Gotoh, Y.; Istomin, V.; Chuvilin, E.; Sakagami, H.; Hachikubo, A. Methane clathrate hydrates formed within hydrophilic and hydrophobic media: Kinetics of dissociation and distortion of host structure. *J. Phys. Chem. C* **2013**, *117*, 7081–7085. [[CrossRef](#)]
108. Falenty, A.; Kuhs, W.F. “Self-Preservation” of CO<sub>2</sub> Gas Hydrates-Surface Microstructure and Ice Perfection. *J. Phys. Chem. B* **2009**, *113*, 15975–15988. [[CrossRef](#)] [[PubMed](#)]
109. Misyura, S.Y.; Donskoy, I.G. Methane hydrate combustion by using different granules composition. *Fuel Process. Technol.* **2017**, *158*, 154–162. [[CrossRef](#)]
110. Misyura, S.Y. Dissociation of various gas hydrates (methane hydrate, double gas hydrates of methane-propane and methane-isopropanol) during combustion: Assessing the combustion efficiency. *Energy* **2020**, *206*, 118120. [[CrossRef](#)]
111. Misyura, S.Y.; Donskoy, I.G. Dissociation and Combustion of a Layer of Methane Hydrate Powder: Ways to Increase the Efficiency of Combustion and Degassing. *Energies* **2021**, *14*, 4855. [[CrossRef](#)]
112. Hassanpouryouzband, A.; Joonaki, E.; Farahani, M.V.; Takeya, S.; Ruppel, C.; Yang, J.; English, N.J.; Schicks, J.M.; Edlmann, K.; Mehrabian, H.; et al. Gas hydrates in sustainable chemistry. *Chem. Soc. Rev.* **2020**, *49*, 5225–5309. [[CrossRef](#)]
113. Vlasov, V.A. Diffusion-kinetic model of gas hydrate film growth along the gas–water interface. *Heat Mass Transf.* **2019**, *55*, 3537–3545. [[CrossRef](#)]
114. Boswell, R.; Shipp, C.; Reichel, T.; Shelander, D.; Saeki, T.; Frye, M.; Shedd, W.; Collett, T.S.; McConnell, D.R. Prospecting for marine gas hydrate resources. *Interpretation* **2016**, *4*, SA13–SA24. [[CrossRef](#)]
115. Lee, M.W.; Dillon, W.P. Amplitude blanking related to the pore-filling of gas hydrate in sediments. *Mar. Geophys. Res.* **2001**, *22*, 101–109. [[CrossRef](#)]
116. Ross Chapman, N.; Gettrust, J.F.; Walia, R.; Hannay, D.; Spence, G.D.; Wood, W.T.; Hyndman, R.D. High-resolution, deep-towed, multichannel seismic survey of deep-sea gas hydrates off western Canada. *Geophysics* **2002**, *67*, 1038–1047. [[CrossRef](#)]
117. Yi, B.Y.; Yoon, Y.H.; Kim, Y.J.; Kim, G.Y.; Joo, Y.H.; Kang, N.K.; Kim, J.K.; Chun, J.H.; Yoo, D.G. Characterization of thin gas hydrate reservoir in ulleung basin with stepwise seismic inversion. *Energies* **2021**, *14*, 4077. [[CrossRef](#)]
118. Li, G.; Li, B.; Li, X.S.; Zhang, Y.; Wang, Y. Experimental and numerical studies on gas production from methane hydrate in porous media by depressurization in pilot-scale hydrate simulator. *Energy Fuels* **2012**, *26*, 6300–6310. [[CrossRef](#)]
119. Li, G.; Moridis, G.J.; Zhang, K.; Li, X. Sen Evaluation of gas production potential from marine gas hydrate deposits in shenhu area of south china sea. *Energy Fuels* **2010**, *24*, 6018–6033. [[CrossRef](#)]
120. Moridis, G.J.; Kowalsky, M.B.; Preuss, K. Depressurization-induced gas production from class 1 hydrate deposits. *SPE Reserv. Eval. Eng.* **2007**, *10*, 458–481. [[CrossRef](#)]

121. Schicks, J.M.; Spangenberg, E.; Giese, R.; MLuzi-Helbin, M.; Priegnitz, M.; Beeskow-Strauch, B. A counter-current heat-exchange reactor for the thermal stimulation of hydrate-bearing sediments. *Energies* **2013**, *6*, 3002–3016. [[CrossRef](#)]
122. Linga, P.; Haligva, C.; Nam, S.C.; Ripmeester, J.A.; Englezos, P. Recovery of Methane from Hydrate Formed in a Variable Volume Bed of Silica Sand Particles. *Energy Fuels* **2009**, *23*, 5508–5516. [[CrossRef](#)]
123. Feng, J.C.; Wang, Y.; Li, X.S.; Li, G.; Chen, Z.Y. Production behaviors and heat transfer characteristics of methane hydrate dissociation by depressurization in conjunction with warm water stimulation with dual horizontal wells. *Energy* **2015**, *79*, 315–324. [[CrossRef](#)]
124. Feng, J.-C.; Li, G.; Li, X.-S.; Li, B.; Chen, Z.-Y. Evolution of Hydrate Dissociation by Warm Brine Stimulation Combined Depressurization in the South China Sea. *Energies* **2013**, *6*, 5402–5425. [[CrossRef](#)]
125. Li, G.; Wu, D.; Li, X.; Zhang, Y.; Lv, Q.; Wang, Y. Experimental Investigation into the Production Behavior of Methane Hydrate under Methanol Injection in Quartz Sand. *Energy Fuels* **2017**, *31*, 5411–5418. [[CrossRef](#)]
126. Chong, Z.R.; Yin, Z.; Tan, J.H.C.; Linga, P. Experimental investigations on energy recovery from water-saturated hydrate bearing sediments via depressurization approach. *Appl. Energy* **2017**, *204*, 1513–1525. [[CrossRef](#)]
127. Yuan, Q.; Sun, C.-Y.; Yang, X.; Ma, P.-C.; Ma, Z.-W.; Li, Q.-P.; Chen, G.-J. Gas Production from Methane-Hydrate-Bearing Sands by Ethylene Glycol Injection Using a Three-Dimensional Reactor. *Energy Fuels* **2011**, *25*, 3108–3115. [[CrossRef](#)]
128. Konno, Y.; Fujii, T.; Sato, A.; Akamine, K.; Naiki, M.; Masuda, Y.; Yamamoto, K.; Nagao, J. Key Findings of the World's First Offshore Methane Hydrate Production Test off the Coast of Japan: Toward Future Commercial Production. *Energy Fuels* **2017**, *31*, 2607–2616. [[CrossRef](#)]
129. Yamamoto, K.; Kanno, T.; Wang, X.X.; Tamaki, M.; Fujii, T.; Chee, S.S.; Wang, X.W.; Pimenov, V.; Shako, V. Thermal responses of a gas hydrate-bearing sediment to a depressurization operation. *RSC Adv.* **2017**, *7*, 5554–5577. [[CrossRef](#)]
130. Javanmardi, J.; Nasrifar, K.; Najibi, S.H.; Moshfeghian, M. Economic evaluation of natural gas hydrate as an alternative for natural gas transportation. *Appl. Therm. Eng.* **2005**, *25*, 1708–1723. [[CrossRef](#)]
131. Song, Y.M.; Liang, R.Q.; Wang, F.; Zhang, D.H.; Yang, L.; Zhang, D.B. Enhanced methane hydrate formation in the highly dispersed carbon nanotubes-based nanofluid. *Fuel* **2021**, *285*, 119234. [[CrossRef](#)]
132. Song, M.H.; Kim, H.S.; Kim, B.M. Influence of production parameters on gas hydrate and ice powder pelletizing. *J. Mech. Sci. Technol.* **2015**, *29*, 1181–1186. [[CrossRef](#)]
133. Mimachi, H.; Takahashi, M.; Takeya, S.; Gotoh, Y.; Yoneyama, A.; Hyodo, K.; Takeda, T.; Murayama, T. Effect of Long-Term Storage and Thermal History on the Gas Content of Natural Gas Hydrate Pellets under Ambient Pressure. *Energy Fuels* **2015**, *29*, 4827–4834. [[CrossRef](#)]
134. Lee, Y.; Seo, Y.J.; Ahn, T.; Lee, J.; Lee, J.Y.; Kim, S.J.; Seo, Y. CH<sub>4</sub>-Flue gas replacement occurring in sH hydrates and its significance for CH<sub>4</sub> recovery and CO<sub>2</sub> sequestration. *Chem. Eng. J.* **2017**, *308*, 50–58. [[CrossRef](#)]
135. Xu, C.-G.; Li, X.-S. Research progress of hydrate-based CO<sub>2</sub> separation and capture from gas mixtures. *RSC Adv.* **2014**, *4*, 18301–18316. [[CrossRef](#)]
136. Ye, J.; Qin, X.; Xie, W.; Lu, H.; Ma, B.; Qiu, H.; Liang, J.; Lu, J.; Kuang, Z.; Lu, C.; et al. The second natural gas hydrate production test in the South China Sea. *China Geol.* **2020**, *3*, 197–209. [[CrossRef](#)]
137. Koh, C.A.; Sum, A.K.; Sloan, E.D. State of the art: Natural gas hydrates as a natural resource. *J. Nat. Gas Sci. Eng.* **2012**, *8*, 132–138. [[CrossRef](#)]
138. Sahoo, M.; Dey, S. A comparative study on the characterisation and combustion behaviour of high ash coals from two different geographical origins. *Fuel* **2021**, *286*, 119397. [[CrossRef](#)]
139. Turns, S.R. *An Introduction to Combustion: Concepts and Applications*, 3rd ed.; McGraw-Hill Education: New York, NY, USA, 2000.
140. Gao, J.; Hossain, A.; Nakamura, Y. Flame base structures of micro-jet hydrogen/methane diffusion flames. *Proc. Combust. Inst.* **2017**, *36*, 4209–4216. [[CrossRef](#)]
141. Maruyama, Y.; Fuse, M.J.; Yokomori, T.; Ohmura, R.; Watanabe, S.; Iwasaki, T.; Iwabuchi, W.; Ueda, T. Experimental investigation of flame spreading over pure methane hydrate in a laminar boundary layer. *Proc. Combust. Inst.* **2013**, *34*, 2131–2138. [[CrossRef](#)]
142. Nakamura, Y.; Katsuki, R.; Yokomori, T.; Ohmura, R.; Takahashi, M.; Iwasaki, T.; Uchida, K.; Ueda, T. Combustion characteristics of methane hydrate in a laminar boundary layer. *Proc. Energy Fuels* **2009**, *23*, 1445–1449. [[CrossRef](#)]
143. Lee, S.; Padilla, R.; Dunn-Rankin, D.; Pham, T.; Kwon, O.C. Extinction limits and structure of counterflow nonpremixed H<sub>2</sub>O-laden CH<sub>4</sub>/air flames. *Energy* **2015**, *93*, 442–450. [[CrossRef](#)]
144. Misyura, S.Y.; Donskoy, I.G. Dissociation of natural and artificial gas hydrate. *Chem. Eng. Sci.* **2016**, *148*, 65–77. [[CrossRef](#)]
145. Bozhko, Y.Y.; Subbotin, O.S.; Gets, K.V.; Zhdanov, R.K.; Belosludov, V.R. Simulation of thermobaric conditions of the formation, composition, and structure of mixed hydrates containing xenon and nitrous oxide. *J. Struct. Chem.* **2017**, *58*, 853–860. [[CrossRef](#)]
146. Yan, C.; Ren, X.; Cheng, Y.; Song, B.; Li, Y.; Tian, W. Geomechanical issues in the exploitation of natural gas hydrate. *Gondwana Res.* **2020**, *81*, 403–422. [[CrossRef](#)]